Vietnam Journal of Mechanics, Vietnam Academy of Science and Technology
DOI: https://doi.org/10.15625/0866-7136/21925

AN APPLICATION OF THE DYNAMIC STIFFNESS CONCEPT FOR VIBRATION OF THREE-DIMENSIONAL CRACKED OVERHEAD CRANE

Dang Xuan Trong[1,*], **Nguyen Tien Khiem**[2]
[1]*Occupational Safety and Health Inspection and Training Joint Stock Company, 733 Xo Viet Nghe Tinh street, Binh Thanh district, Ho Chi Minh City, Vietnam*
[2]*Institute of Mechanics, VAST, 264 Doi Can street, Ba Dinh district, Hanoi, Vietnam*
*E-mail: dotrongatldtp@yahoo.com

Received: 25 September 2024 / Revised: 01 October 2024 / Accepted: 12 October 2024
Published online: 15 October 2024

Abstract. A simplified model is proposed for modal analysis of cracked 3D-framed overhead crane of H-form frame using the well-known dynamic stiffness method. First, the dynamic stiffness of a cracked beam is derived as the inverse of the frequency response function and used for establishing a model of the cracked beam called dynamic stiffness one. Then, the dynamic stiffness model of cracked beams is employed for representing two supporting beams in the H-form frame crane. So that a simplified model of the overhead crane is conducted as a beam with artificial elastic supports of stiffness obtained above for supporting beam. Finally, the free vibration problem of the simplified overhead crane is formulated and solved for the crane fundamental frequency analysis in dependence upon crack parameters and supporting positions. Numerical computation is accomplished for illustrating the proposed theory and providing some conclusions on the simplified model of 3D overhead cranes.

Keywords: overhead crane, cracked frame, dynamic stiffness, free vibration.

1. INTRODUCTION

Cranes are very important instruments in construction and transportation and dynamic analysis of such structures is truly vital in both stages of designing and operating, especially for the massive cranes [1]. Dynamic analysis of cranes is required not only to evaluate the dynamic load capacity but also for their control and health monitoring [2]. Cranes may be classified into three classes: overhead (gantry), tower (rotary), and mobile (boom) cranes (see Fig. 1); however, overhead cranes are the most gigantic and widely used in industry for the transportation of heavy loads. The fundamental problems of modeling and control of overhead cranes were presented in [3]. The dynamics of an overhead crane in the simplest model were studied in [4], in which the supporting structure is ignored, and the crane is treated as a simply supported beam with a pendulum moving on it. This is only a planar model of overhead cranes.

(a) Overhead (b) Tower (c) Mobile

Fig. 1. Typical cranes

The modeling, control, and dynamics of three-dimensional overhead cranes were investigated in [5, 6], where, however, the authors focused only on the three-dimensional motion of the pendulum. The dynamics of a three-dimensional overhead crane with an elastic framed supporting structure were studied in [7] by using the finite element method (FEM). Natural frequencies of the 3D-framed overhead crane computed by FEM in this work were compared to experimental results. However, the difference between FEM-computed and measured natural frequencies is shown to be large, more than 20%. The so-called dynamic stiffness method (DSM) is an alternative technique that could significantly improve the FEM in the dynamic analysis of frame structures [8], especially, for cracked structures [9, 10]. Nevertheless, the DSM has been used only for dynamic analysis of tower cranes with cracks in [11–13].

Thus, in the present study, the DSM is developed for modal analysis of cracked 3D-framed overhead crane of H-form as shown in Fig. 2. First, the dynamic stiffness of a cracked beam is derived as the inverse of the frequency response function [14] and used for establishing a model of the cracked beam called dynamic stiffness model. Then, the dynamic stiffness model of cracked beams is employed for representing two supporting beams in the frame crane shown in Fig. 2. So that a simplified model of the overhead crane is conducted as a beam with artificial elastic supports of stiffness obtained above for supporting beams (Fig. 3). Finally, free vibration problem of the simplified overhead crane is formulated and solved to analyze the crane fundamental frequency in dependence upon crack parameters and supporting positions. Numerical computation is accomplished for illustrating the proposed theory and providing some conclusions on the use of the simplified model of 3D overhead cranes.

2. A SIMPLIFIED MODEL OF OVERHEAD CRANE

Let's consider an overhead crane given in Fig. 2 composed of three connected beams AB, CD, and EF. The first two beams AB and CD are parallel rails, and the third beam EF is perpendicular to AB and CD served as bridging crane beam. This framed structure can be easily modeled by either the conventional finite element method [10] or the dynamic stiffness technique [9]. However, neither of the well-known methods including the ones mentioned above can result in an analytical solution to the vibration problem of the 3D-frame structure simply like that solution obtained for a single beam. Thus, in the present section, we propose an approach to simplify the 3D frame structure to a beam structure so that its vibration problem can be easily solved by the classical analytical method.

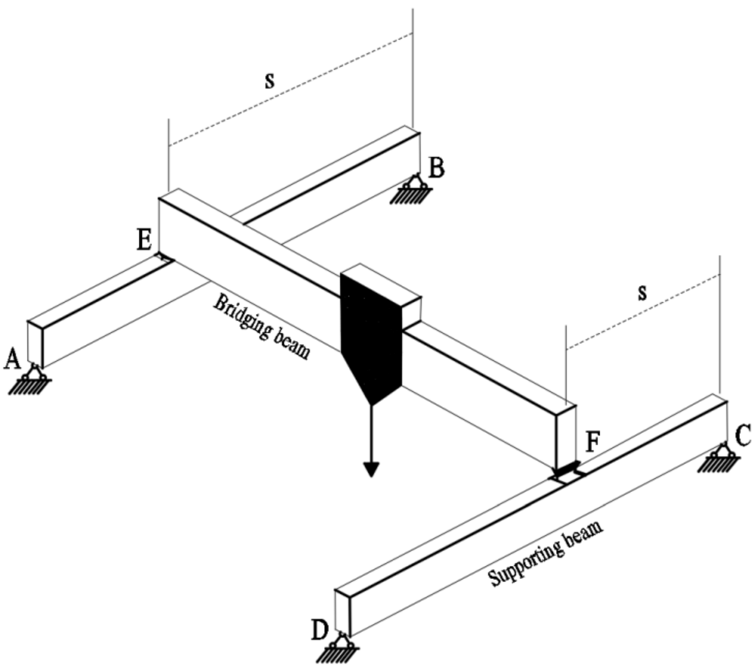

Fig. 2. Model of an overhead bridge crane

As shown in Fig. 2, the EF beam is rested on the elastic beams AB and CD at its ends, and they are all together vibrating as members of the total frame. Therefore, it can be treated that the EF beam is rested on elastic boundary supports at the position s on the AB and CD beams measured from their origins B and C. The equivalent model of the overhead crane is shown in Fig. 3, where the question is how to select an equivalent stiffness for the elastic end supports to represent the supporting beams adequately. Conventionally, the stiffness of the elastic supports is selected as the static stiffness of the beams at a given position, and it can be calculated by a classical method of the structural mechanics. However, this selection ignores the inertia of the supporting beams under vibration, and it is difficult to choose for the case when the supporting beams contain damages such as cracks. We propose in this study to select the dynamic stiffness of the beams at the supporting point that can be constructed in the subsequent section for multiple cracked beams.

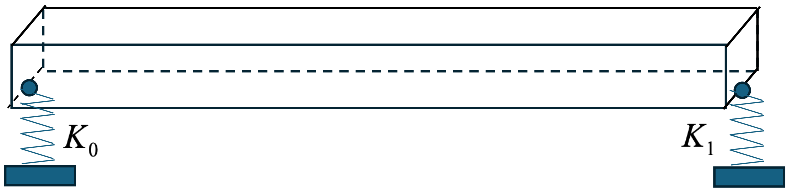

Fig. 3. Reduced model of overhead crane

Thus, considering mechanical system given in Fig. 3, where two springs supporting the beam have dynamic stiffness K_0, K_1 respectively. As it is well known that under harmonic forces of frequency ω and amplitudes $P_0(\omega), P_1(\omega)$ the springs undergo the displacements of amplitudes $w_0(\omega), w_1(\omega)$ satisfying the relationship

$$P_0 = K_0 w_0, \quad P_1 = K_1 w_1.$$

On the other hand, for the beam vibrating with boundary deflection amplitudes denoted by $w_0 = W(\omega, 0), w_1 = W(\omega, L)$, the corresponding shear forces are determined as

$$P_0(\omega) = -EIW'''(\omega, 0), \quad P_1(\omega) = EIW'''(\omega, L).$$

Hence, boundary conditions for the beam given in Fig. 3 should be

$$EIW'''(\omega, 0) + K_{AB}(\omega, \overline{x}) W(\omega, 0) = 0, \quad EIW'''(\omega, L) - K_{CD}(\omega, \overline{x}) W(\omega, L) = 0, \quad (1)$$

with $K_{AB}(\omega, \overline{x})$ and $K_{CD}(\omega, \overline{x})$ being dynamic stiffness of AB and CD beams calculated at position $\overline{x}$. The next section is devoted to constructing the dynamic stiffness of AB and CD beams with cracks.

3. DYNAMIC STIFFNESS MODEL OF MULTIPLE CRACKED BEAM

It is well known that vibration of Euler–Bernoulli beam subjected to a force concentrated at position x_0, described by the equation [10]

$$EI\partial^4 W\left(x,t\right)/\partial x^4 + \rho F \partial^2 W\left(x,t\right)/\partial t^2 = P\left(t\right)\delta\left(x-x_0\right),$$

that is transformed into the frequency domain equation

$$EI\mathrm{d}^4\Phi\left(x,\omega\right)/\mathrm{d}x^4 - \rho F\omega^2\Phi\left(x,\omega\right) = Q\left(\omega\right)\delta\left(x-x_0\right). \tag{2}$$

Using the notation

$$\lambda = \left(\rho A L^4\omega^2/EI\right)^{1/4}, \quad Q_0\left(\omega\right) = Q\left(\omega\right)/EI,$$

Eq. (2) can be rewritten in the form

$$\mathrm{d}^4\Phi\left(x,\omega\right)/\mathrm{d}x^4 - \lambda^4\Phi\left(x,\omega\right) = Q_0\left(\omega\right)\delta\left(x-x_0\right), \quad x\in[0,1]. \tag{3}$$

For the beam cracked at positions $0 < e_1 < \ldots < e_n < 1$, general solution of the equation

$$\mathrm{d}^4\Phi\left(x,\omega\right)/\mathrm{d}x^4 - \lambda^4\Phi\left(x,\omega\right) = 0, \tag{4}$$

denoted by $\Phi_0\left(x,\omega\right)$ can be represented by [10]

$$\Phi_0\left(x,\omega\right) = C_1\Phi_1\left(x,\omega\right) + C_2\Phi_2\left(x,\omega\right), \tag{5}$$

where

$$\begin{aligned}\Phi_1\left(x,\omega\right) &= L_1\left(x,\lambda\right) + \sum_{j=1}^{n}\mu_{1k}K\left(x-e_j,\lambda\right),\\ \Phi_2\left(x,\omega\right) &= L_2\left(x,\lambda\right) + \sum_{j=1}^{n}\mu_{2k}K\left(x-e_j,\lambda\right),\end{aligned} \tag{6}$$

with the vectors of damage parameters $\mu_1 = \left(\mu_{11},\ldots,\mu_{1n}\right)^T, \mu_2 = \left(\mu_{21},\ldots,\mu_{2n}\right)^T$ determined from crack magnitudes $\gamma_j, j = 1,2,\ldots,n$ as

$$\mu_{1j} = \gamma_j\left[L_1''\left(e_j,\lambda\right) + \sum_{k=1}^{j-1}\mu_{1k}S''\left(e_j-e_k,\lambda\right)\right],$$

$$\mu_{2j} = \gamma_j\left[L_2''\left(e_j,\lambda\right) + \sum_{k=1}^{j-1}\mu_{2k}S''\left(e_j-e_k,\lambda\right)\right],$$

and

$$K\left(x,\lambda\right) = \begin{cases}0, & x\le 0\\ S(x,\lambda), & x>0\end{cases}, \quad S\left(x,\lambda\right) = \left[\sinh\lambda x + \sin\lambda x\right]/2\lambda.$$

Table 1. Boundary condition functions

Boundary Conditions	$L_1\left(x,\lambda\right)$	$L_2\left(x,\lambda\right)$	p	q
Clamped end	$\sinh\lambda x - \sin\lambda x$	$\cosh\lambda x - \cos\lambda x$	0	1
Free end	$\sinh\lambda x + \sin\lambda x$	$\cosh\lambda x + \cos\lambda x$	2	3
Hinged support	$\sin\lambda x$	$\sinh\lambda x$	0	2

Assuming furthermore that functions $L_1(x,\lambda), L_2(x,\lambda)$ in (5)–(6) are solutions of Eq. (4) satisfying boundary conditions at the left end, $x = 0$, that are given in Table 1 for conventional boundary conditions.

Next, according to the theory of differential equations, general solution of inhomogeneous equation (3) can be expressed as

$$\Phi(x,\omega) = \Phi_0(x,\omega) + Q_0(\omega) H(x - x_0,\lambda), \tag{7}$$

where

$$H(x,\lambda) = \begin{cases} 0, & \text{when } x \le x_0 \\ h(x,\lambda), & \text{when } x > x_0 \end{cases}, \quad h(x,\lambda) = [\sinh\lambda x - \sin\lambda x]/2\lambda^3.$$

Substituting solution (7) into boundary conditions at the beam end, $x = 1$, that is represented by

$$\Phi^{(p)}(1,\omega) = \Phi^{(q)}(1,\omega) = 0,$$

where p, q are given also in Table 1, one obtains equations for determining constants C_1, C_2 as

$$\begin{cases} C_1\Phi_1^{(p)}(1,\omega) + C_2\Phi_2^{(p)}(1,\omega) = -Q_0(\omega) h^{(p)}(1 - x_0,\lambda), \\ C_1\Phi_1^{(q)}(1,\omega) + C_2\Phi_2^{(q)}(1,\omega) = -Q_0(\omega) h^{(q)}(1 - x_0,\lambda). \end{cases}$$

It is easily to verify that the latter equations give rise the solution

$$C_1 = Q_0\overline{C}_1/D, \quad C_2 = Q_0\overline{C}_1/D,$$

where the coefficients

$$\begin{aligned} D(\omega) &= \Phi_1^{(p)}(1,\omega)\Phi_2^{(q)}(1,\omega) - \Phi_1^{(q)}(1,\omega)\Phi_2^{(p)}(1,\omega), \\ \overline{C}_1 &= h^{(q)}(1 - x_0,\lambda)\Phi_2^{(p)}(1,\omega) - h^{(p)}(1 - x_0,\lambda)\Phi_2^{(q)}(1,\omega), \\ \overline{C}_2 &= h^{(p)}(1 - x_0,\lambda)\Phi_1^{(q)}(1,\omega) - h^{(q)}(1 - x_0,\lambda)\Phi_1^{(p)}(1,\omega). \end{aligned}$$

Thus, solution (7) can be rewritten as

$$\begin{aligned} \Phi(x,\omega) = Q_0(\omega)\big\{H(x - x_0,\lambda) + \big[\overline{C}_1(x_0,\omega)\Phi_1(x,\omega) \\ + \overline{C}_2(x_0,\omega)\Phi_2(x,\omega)\big]/D(\omega)\big\}. \end{aligned}$$

Therefore, the frequency response function defined as $\Phi(x,\omega)/Q(\omega)$, can be obtained in the form [14]

$$\begin{aligned} FRF(x,x_0,\omega) = (1/EI)\big\{H(x - x_0,\lambda) + \big[\overline{C}_1(x_0,\omega)\Phi_1(x,\omega) \\ \overline{C}_2(x_0,\omega)\Phi_2(x,\omega)\big]/D(\omega)\big\}. \end{aligned}$$

On the other hand, the so-called dynamic stiffness of the beam is defined as $K(\omega, x, x_0) = 1/FRF(\omega, x, x_0)$ or

$$K(\omega, x, x_0) = EI \times D(\omega) \;/\; [H(x - x_0, \lambda) D(\omega) + \overline{C}_1(x_0, \omega) \Phi_1(x, \omega) + \overline{C}_2(x_0, \omega) \Phi_2(x, \omega)] .$$

In case, if $x_0 = x = s$ (acknowledged herein as driven collocation) the dynamic stiffness gets to be

$$K(\omega, s) = EI \times D(\omega) \;/\; \left[\overline{C}_1(s, \omega) \Phi_1(s, \omega) + \overline{C}_2(a, \omega) \Phi_2(s, \omega)\right] . \tag{8}$$

Now, we consider specifically the case of beam with single crack of magnitude γ at position e that gives Eq. (8) reduced to

$$K(\omega, s, e) = EI\,[D_0(\lambda) + \gamma D_c(\lambda, e)] \;/\; [F_0(\lambda, s) + \gamma F_c(\lambda, s, e)] ,$$

where

$$\begin{aligned}
D_0(\lambda) &= L_1^{(p)}(1) L_2^{(q)}(1) - L_2^{(p)}(1) L_1^{(q)}(1) , \\
F_0(\lambda, x) &= C_{10}(x) L_1(x) + C_{20}(x) L_2(x) , \\
D_c(\lambda, e) &= \left[L_2^{(q)}(1) L_1''(e) - L_1^{(q)}(1) L_2''(e)\right] S^{(p)}(1 - e) \\
&\quad + \left[L_1^{(p)}(1) L_2''(e) - L_2^{(p)}(1) L_1''(e)\right] S^{(q)}(1 - e) , \\
F_c(\lambda, s, e) &= \left[C_{10}(s) L_1''(e) + C_{20}(x) L_2''(e)\right] K(s - e) \\
&\quad + \left[L_1(s) L_2''(e) - L_2(s) L_1''(e)\right] C_{12}(s, e) , \\
C_{10}(s) &= h^{(q)}(1 - s) L_2^{(p)}(1) - h^{(p)}(1 - s) L_2^{(q)}(1) , \\
C_{20}(s) &= h^{(p)}(1 - s) L_1^{(q)}(1) - h^{(q)}(1 - s) L_1^{(p)}(1) , \\
C_{12}(s, e) &= h^{(q)}(1 - s) S^{(p)}(1 - e) - h^{(p)}(1 - s) S^{(q)}(1 - e) .
\end{aligned}$$

For simply supported beam when $L_1(x, \lambda) = \sin \lambda x, L_2(x, \lambda) = \sinh \lambda x, p = 0, q = 2$ one obtains

$$\begin{aligned}
D_0(\lambda) &= 2\lambda^2 \sinh \lambda \sin \lambda, \\
F_0(\lambda, s) &= (1/\lambda)\,[\sinh \lambda \sin \lambda (1 - s) \sin \lambda s - \sin \lambda \sinh \lambda (1 - s) \sinh \lambda s] , \\
D_c(\lambda, e) &= -\lambda^3 \sin \lambda (1 - e)\,[\sinh \lambda \sin \lambda e + \sin\lambda \sinh \lambda e] , \\
F_c(\lambda, s, e) &= \lambda\,[D_1(\lambda, s, e) - D_0(\lambda, s, e) K(s - e)] ,
\end{aligned}$$

with

$$\begin{aligned}
D_1(\lambda, s, e) &= (1/2) \begin{bmatrix} \sinh \lambda e \sin \lambda (1 - e) \sinh \lambda (1 - e) \sin \lambda s \\ + \sinh \lambda e \sinh \lambda (1 - e) \sin \lambda (1 - s) \sin \lambda s \\ + \sin \lambda e \sin \lambda (1 - e) \sinh \lambda (1 - s) \sinh \lambda s \\ + \sin \lambda e \sinh \lambda (1 - e) \sin \lambda (1 - s) \sinh \lambda s \end{bmatrix} , \\
D_0(\lambda, s, e) &= \sinh \lambda \sin \lambda e \sin \lambda (1 - s) + \sin \lambda \sinh \lambda e \sinh \lambda (1 - s) .
\end{aligned}$$

Moreover, for uncracked simply supported beam the dynamic stiffness gets to be

$$K(\omega, s) = 2EI\lambda^3 \sinh\lambda \sin\lambda / \left[\sinh\lambda \sin\lambda(1-s)\sin\lambda s - \sin\lambda \sinh\lambda(1-s)\sinh\lambda s\right].$$

Particularly, the dynamic stiffness at the beam middle ($s = 1/2$) is

$$K_{L/2}(\omega) = 4EI\lambda^3 / \left[\tan\lambda/2 - \tanh\lambda/2\right]. \tag{9}$$

From (9) it can be easy to calculate the limit:

$$\lim_{\omega\to 0} K_{L/2}(\omega) = 48EI/L^3,$$

that is static stiffness calculated at the middle of a simply supported beam in the structural mechanics [9].

4. VIBRATION OF CRACKED OVERHEAD CRANE

4.1. Vibration shape of cracked overhead crane

Consider now an overhead crane modeled by a simple beam supported on artificial springs of dynamic stiffness K_0, K_1 calculated by formulae (8) for two supporting beams. In that case, since boundary conditions (1) are not conventional, general solution of Eq. (4) must be expressed in the form [10]

$$\Phi_0(x,\omega) = C_1\Phi_1(x,\omega) + C_2\Phi_2(x,\omega) + C_3\Phi_3(x,\omega) + C_4\Phi_4(x,\omega), \tag{10}$$

where

$$\Phi_1(x,\omega) = L_1(x,\lambda) + \sum_{j=1}^{n}\mu_{1j}K\left(x - e_j, \lambda\right),$$

$$\Phi_2(x,\omega) = L_2(x,\lambda) + \sum_{j=1}^{n}\mu_{2j}K\left(x - e_j, \lambda\right)$$

$$\Phi_3(x,\omega) = L_3(x,\lambda) + \sum_{j=1}^{n}\mu_{3j}K\left(x - e_j, \lambda\right),$$

$$\Phi_4(x,\omega) = L_4(x,\lambda) + \sum_{j=1}^{n}\mu_{4j}K\left(x - e_j, \lambda\right)$$

with functions

$$L_1(x) = (\sinh\lambda x + \sin\lambda x)/2, \quad L_2(x) = (\cosh\lambda x + \cos\lambda x)/2,$$
$$L_3(x) = (\sinh\lambda x - \sin\lambda x)/2, \quad L_4(x) = (\cosh\lambda x - \cos\lambda x)/2,$$
$$K(x,\lambda) = \begin{cases} 0, & x \le 0 \\ S(x,\lambda), & x > 0 \end{cases}, \quad K'(x,\lambda) = \begin{cases} 0, & x \le 0 \\ S'(x,\lambda), & x > 0 \end{cases},$$
$$K''(x,\lambda) = \begin{cases} 0, & x \le 0 \\ S''(x,\lambda), & x > 0 \end{cases}, \quad S(x,\lambda) = \left[\sinh\lambda x + \sin\lambda x\right]/2\lambda,$$

and damage parameters $\mu_k = (\mu_{k1}, \ldots, \mu_{kn})^T, k = 1,2,3,4$ determined by

$$\mu_{ij} = \gamma_j \left[L_i'' \left(e_j, \lambda\right) + \sum_{k=1}^{j-1} \mu_{jk} S'' \left(e_j - e_k, \lambda\right) \right], \quad i = 1,2,3,4.$$

Following the simplified model of the overhead crane under consideration, the solution (10) must satisfy the boundary conditions

$$\begin{aligned} EI\Phi'' (0, \omega) &= EI\Phi''' (0, \omega) + K_0 (\omega) \Phi (0, \omega) = 0, \\ EI\Phi'' (1, \omega) &= EI\Phi''' (1, \omega) - K_1 (\omega) \Phi (1, \omega) = 0, \end{aligned}$$

or

$$\begin{aligned} \Phi'' (0, \omega) &= \Phi''' (0, \omega) + \overline{K}_0 (\omega) \Phi (0, \omega) = 0, \\ \Phi'' (1, \omega) &= \Phi''' (1, \omega) - \overline{K}_1 (\omega) \Phi (1, \omega) = 0, \end{aligned} \tag{11}$$

where

$$\overline{K}_0 = K_0 (\omega) / EI, \quad \overline{K}_1 = K_1 (\omega) / EI.$$

4.2. Free vibration of overhead crane with cracks

Thus, satisfying solution (10) with boundary conditions (11) yields the system of equations with respect to constants $C_1, \ldots, C_4$ as

$$\begin{aligned} & C_1 \Phi_1'' (0, \omega) + C_2 \Phi_2'' (0, \omega) + C_3 \Phi_3'' (0, \omega) + C_4 \Phi_4'' (0, \omega) = 0, \\ & C_1 \left[\Phi_1''' (0, \omega) + \overline{K}_0 \Phi_1 (0, \omega)\right] + C_2 \left[\Phi_2''' (0, \omega) + \overline{K}_0 \Phi_2 (0, \omega)\right] \\ & \qquad + C_3 \left[\Phi_3''' (0, \omega) + \overline{K}_0 \Phi_3 (0, \omega)\right] + C_4 \left[\Phi_4''' (0, \omega) + \overline{K}_0 \Phi_4 (0, \omega)\right] = 0, \\ & C_1 \Phi_1'' (1, \omega) + C_2 \Phi_2'' (1, \omega) + C_3 \Phi_3'' (1, \omega) + C_4 \Phi_4'' (1, \omega) = 0, \\ & C_1 \left[\Phi_1''' (1, \omega) - \overline{K}_1 \Phi_1 (1, \omega)\right] + C_2 \left[\Phi_2''' (1, \omega) - \overline{K}_1 \Phi_2 (1, \omega)\right] \\ & \qquad + C_3 \left[\Phi_3''' (1, \omega) - \overline{K}_1 \Phi_3 (1, \omega)\right] + C_4 \left[\Phi_4''' (1, \omega) + \overline{K}_1 \Phi_4 (1, \omega)\right] = 0, \end{aligned}$$

that can be rewritten in the matrix form

$$[\mathbf{B} (\omega)] \{\mathbf{C}\} = \{\mathbf{0}\},$$

where vector $\{\mathbf{C}\} = \{C_1, \ldots, C_4\}^T$ and matrix **[B]** is

$$[\mathbf{B} (\omega)] = \begin{bmatrix} 0 & 0 & 0 & \lambda^2 \\ 0 & \overline{K}_0 & \lambda^3 & 0 \\ \phi_{31} & \phi_{32} & \phi_{33} & \phi_{34} \\ \phi_{41} & \phi_{42} & \phi_{43} & \phi_{44} \end{bmatrix},$$

in which the following notations have been used

$$
\begin{aligned}
\phi_{31} &= \lambda^2 L_3(1) + \lambda \sum_{k=1}^{n} \mu_{1k} L_3(1-e_k),\\
\phi_{32} &= \lambda^2 L_4(1) + \lambda \sum_{k=1}^{n} \mu_{2k} L_3(1-e_k),\\
\phi_{33} &= \lambda^2 L_1(1) + \lambda \sum_{k=1}^{n} \mu_{3k} L_3(1-e_k),\\
\phi_{34} &= \lambda^2 L_2(1) + \lambda \sum_{k=1}^{n} \mu_{4k} L_3(1-e_k),\\
\phi_{41} &= \left[\lambda^3 L_4(1) - \overline{K}_1 L_1(1)\right] + \sum_{k=1}^{n} \mu_{1k} \Gamma(1-e_k),\\
\phi_{42} &= \left[\lambda^3 L_1(1) - \overline{K}_1 L_2(1)\right] + \sum_{k=1}^{n} \mu_{2k} \Gamma(1-e_k),\\
\phi_{43} &= \left[\lambda^3 L_2(1) - \overline{K}_1 L_3(1)\right] + \sum_{k=1}^{n} \mu_{3k} \Gamma(1-e_k),\\
\phi_{44} &= \left[\lambda^3 L_3(1) - \overline{K}_1 L_4(1)\right] + \sum_{k=1}^{n} \mu_{4k} \Gamma(1-e_k),\\
\Gamma(1-e_k) &= \left[\lambda^2 L_4(1-e_k) - \overline{K}_1 L_1(1-e_k)\right].
\end{aligned}
$$

Therefore, frequency equation for finding natural frequencies of the simplified overhead crane is

$$\det\left[\mathbf{B}(\omega)\right] = 0,$$

that can be expressed in the form

$$D_0(\omega) \equiv \lambda^3 \left(\phi_{31}\phi_{42} - \phi_{41}\phi_{32}\right) - \overline{K}_0 \left(\phi_{31}\phi_{43} - \phi_{41}\phi_{33}\right) = 0. \tag{12}$$

In case of uncracked bridging beam, the latter equation becomes

$$
\begin{aligned}
\lambda^6 \left[L_1(1) L_3(1) - L_4^2(1)\right] - \lambda^3 \left(\overline{K}_0 + \overline{K}_1\right)\left[L_2(1) L_3(1) - L_1(1) L_4(1)\right]&\\
+\overline{K}_0\overline{K}_1 \left[L_3^2(1) - L_1^2(1)\right] = 0,&
\end{aligned} \tag{13}
$$

or

$$
\begin{aligned}
\lambda^6 \left(1 - \cosh\lambda\cos\lambda\right) - \lambda^3 \left(\overline{K}_0 + \overline{K}_1\right)\left(\sinh\lambda\cos\lambda - \cosh\lambda\sin\lambda\right)&\\
+2\overline{K}_0\overline{K}_1 \sinh\lambda\sin\lambda = 0.&
\end{aligned}
$$

Moreover, for the beam with single crack of magnitude γ at position e the frequency equation (12) is

$$
\begin{aligned}
&\left[\lambda^6 d_0(\lambda) - \lambda^3 \left(\overline{K}_0 + \overline{K}_1\right) d_1(\lambda) + \overline{K}_0\overline{K}_1 d_2(\lambda)\right]\\
&\quad + \lambda\gamma \left[\lambda^6 d_0^c(\lambda, e) - \lambda^3 \left(\overline{K}_0 d_{01}^c(\lambda, e) + \overline{K}_1 d_{11}^c(\lambda, e)\right) + \overline{K}_0\overline{K}_1 d_2^c(\lambda, e)\right] = 0,
\end{aligned} \tag{14}
$$

where

$$\begin{aligned}
d_0(\lambda) &= \left[L_1(1)L_3(1) - L_4^2(1)\right],\\
d_1(\lambda) &= \left[L_2(1)L_3(1) - L_1(1)L_4(1)\right],\\
d_2(\lambda) &= L_3^2(1) - L_1^2(1),\\
d_0^c(\lambda, e) &= \{[L_1(1)L_3(e) - L_4(1)L_4(e)]\,L_3(1-e)\\
&\quad + [L_3(1)L_4(e) - L_4(1)L_3(e)]\,L_4(1-e)\},\\
d_{01}^c(\lambda, e) &= \{[L_2(1)L_3(e) - L_4(1)L_1(e)]\,L_3(1-e)\\
&\quad + [L_3(1)L_1(e) - L_1(1)L_3(e)]\,L_4(1-e)\},\\
d_2^c(\lambda, e) &= \{[L_3(1)L_3(e) - L_1(1)L_1(e)]\,L_3(1-e)\\
&\quad + [L_3(1)L_1(e) - L_1(1)L_3(e)]\,L_1(1-e)\},\\
d_{11}^c(\lambda, e) &= [L_4(1)L_3(e) - L_3(1)L_4(e)]\,L_1(1-e).
\end{aligned}$$

It is easy to be verified that under $\gamma = 0$ the equation (14) is reduced to Eq. (13) and a crack abolishes the symmetry of the support stiffness effect.

5. NUMERICAL RESULTS AND DISCUSSION

Numerical results provided in this section are obtained for a frame given in Fig. 2 and represented by its reduced model given in Fig. 3, where two supporting beams AB and CD have been replaced by their dynamic stiffness K_0, K_1. Thus, vibration of the frame overhead crane is now investigated by vibration of bridging beam EF exhibited in Fig. 2. Material and geometry constants of the beams are:

Bridging beam: L = 1 m; b = 0.1 m; h = 0.1 m; E = 200e9 (N/m^2); ρ = 7800 kg/m^3.

Supporting beams: L_{AB} = L_{CD} = 1 m, b_{AB} = b_{CD} = 0.1 m, h_{AB} = h_{CD} = 0.1 m, E_{AB} = E_{CD} = 210e9 (N/m^2), ρ_{AB} = ρ_{AB} = 7855 kg/m^3.

First, we study the dynamic stiffness of the supporting beams as function of frequency in dependence upon crack parameters and supporting points (called above driven positions on supporting beams). Then, the fundamental frequency of the simplified overhead crane is examined along various cracks on either supporting or bridging beams. Boundary conditions of supporting beams are assumed to be hinged supports.

5.1. Dynamic stiffness analysis

The dynamic stiffness of simply supported beams with single crack is calculated versus frequency parameter $\lambda = L\left(\omega^2\rho A/EI\right)^{1/4}$ for various driven points and crack parameters is presented in Figs. 4 and 5. Fig. 4 shows the dynamic stiffness of uncracked (a) and cracked (b) beams in different driven points $s/L = 0.2, 0.3, 0.5, 0.7, 0.8$. It can be seen from Fig. 4(a) that symmetrical driven points give the same dynamic stiffness for uncracked beam, but a crack occurred at the beam destroys the symmetry (Fig. 4(b)). Namely, even a crack at the beam middle makes the dynamic stiffness obtained for symmetrical positions much different excepting the case when dynamic stiffness is defined also at the beam middle. Furthermore, it is observed the well-known fact that the dynamic stiffness vanishes at resonant (natural) frequencies and becomes the infinity (location of vertical lines) at the so-called anti-resonant frequencies [14]. Obviously, resonant frequencies are independent upon position where the dynamic stiffness is measured, for instance, fundamental frequency of simply supported beam is $\lambda_1 = \pi$ which can be clearly seen in Fig. 4(a). While the anti-resonant frequencies are strongly dependent on the position where the dynamic stiffness is determined.

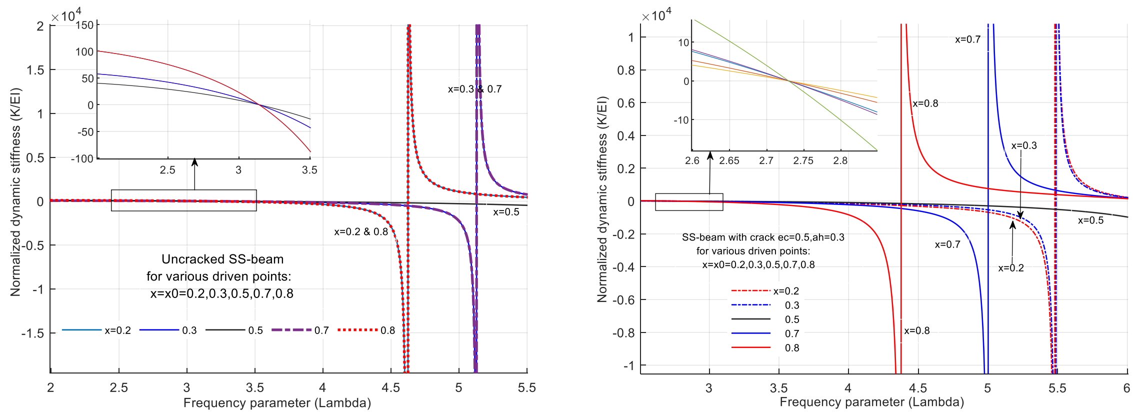

(a) (b)

Fig. 4. Dynamic stiffness of uncracked (a) and cracked (b) beams dependent on driven location. Crack position is the beam middle and crack depth $a/h = 30\%$

Fig. 5 presents the dynamic stiffness in dependence of the crack depth for different combinations of the crack position and driven location: (a) $e = L/2$, $x = L/2$; (b) $e = L/5$, $x = L/5$; (c) $e = L/5$, $x = L/2$ and (d) $e = L/2$, $x = L/5$. It is observed that there is a significant difference between the dynamic stiffness computed at the locations $L/2$ and $L/5$ when the crack occurred at those driven points. The difference is observed by the absence of anti-resonant frequencies (vertical lines) existing when both the crack position and driven location are at the beam middle ($L/2$) (Fig. 5(a)), while all the anti-resonant frequencies appear for the locations at the position $L/5$ (Fig. 5(b)). Finally, all graphs presented in Fig. 5 show the well-known fact that the crack reduces not only the dynamic stiffness of beam but also either resonant frequencies or anti-resonant ones.

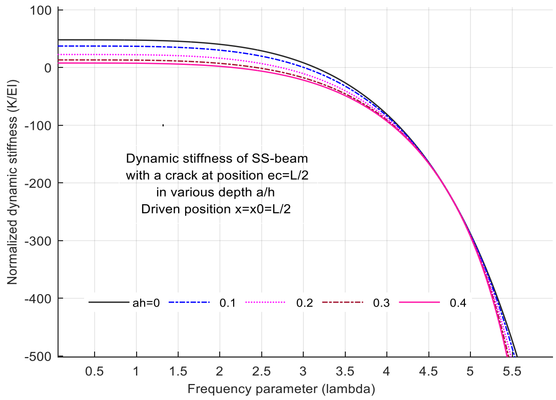

(a) $e/L = 0.5$, $s/L = 0.5$

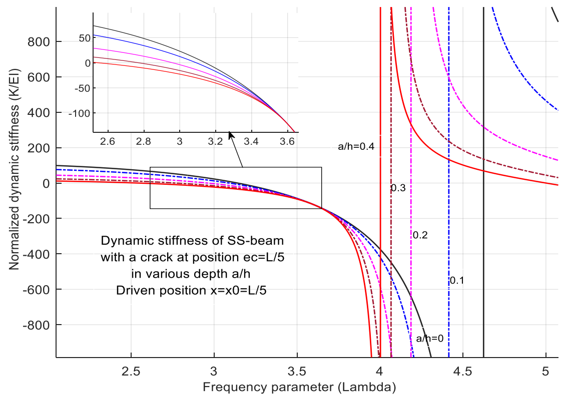

(b) $e/L = 0.2$, $s/L = 0.2$

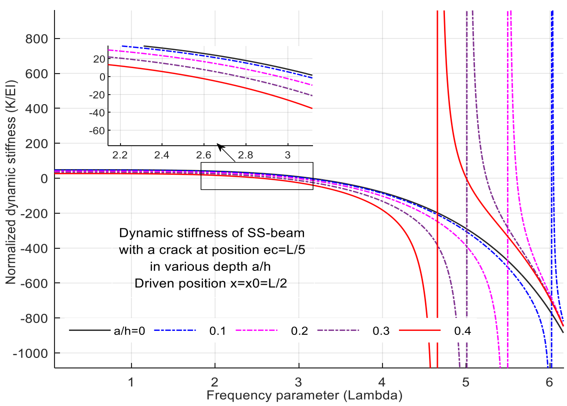

(c) $e/L = 0.2$, $s/L = 0.5$

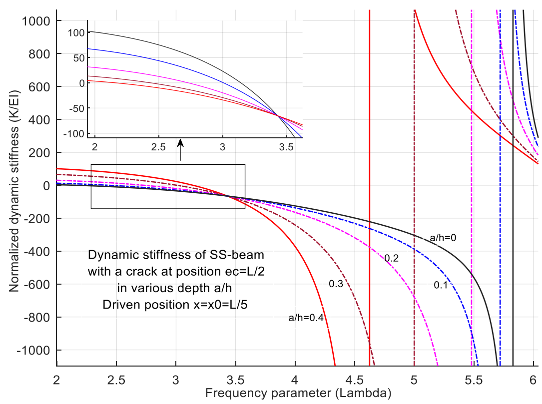

(d) $e/L = 0.5$, $s/L = 0.2$

Fig. 5. Dynamic stiffness of cracked beams computed for various crack depths in different cases of crack location and driven position

5.2. Fundamental frequency of overhead crane

First, to validate the theoretical development proposed above, we have calculated the fundamental frequency of the overhead crane in a particular case when the stiffness of two supports is assumed to be infinite $K_0 = K_1 = \infty$, which results in a fundamental frequency equal to 3.14159 (π). This is the case when the overhead crane is reduced to a simply supported beam.

Next, the fundamental frequency of overhead crane computed along the crack position on the beam members for various crack depths and supporting locations is depicted in Figs. 6–8. Fig. 6 presents the variation of fundamental frequency of overhead crane due to crack occurred in bridging beam in case of uncracked (Fig. 6(a)) and cracked (Fig. 6(b)) supporting beams. Graphs given in Fig. 6(a) exhibit the crack-induced change in fundamental frequency of a beam with artificial elastic supports and show significant effect of the supports compared to those of simply supported beam provided in [10]. Namely, the fundamental frequency of a simply supported beam may decrease by about 12% due to a crack of 40% depth, as seen in [10], while that crack can reduce the fundamental frequency of a beam with artificial elastic supports to 36%. Observing the graphs depicted in Fig. 6(b), one can reveal an interesting fact that a crack in supporting beams could considerably decrease the frequency sensitivity to a crack in the bridging beam. A crack of depth 40% in the supporting beams could reduce the change induced by crack in bridging beam from 36% to 8% (Fig. 6(b)).

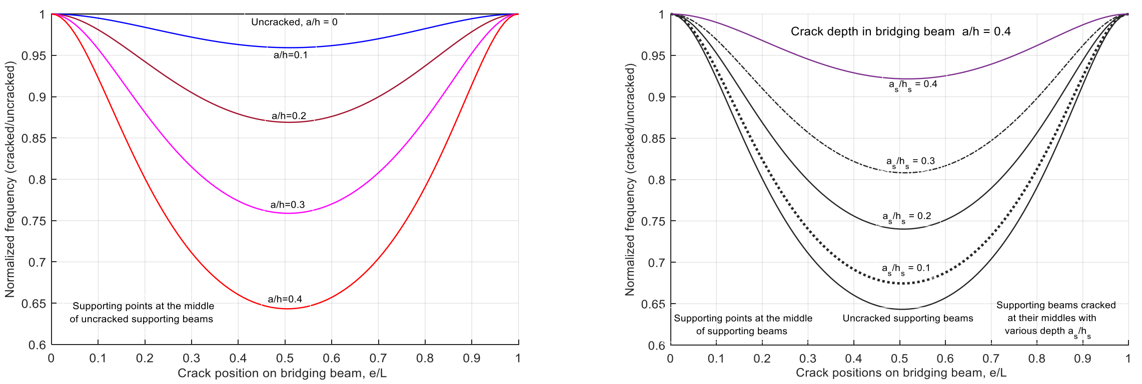

(a) (b)

Fig. 6. Fundamental frequency of overhead crane versus crack position on bridging beam for various (a) depth of crack in bridging beam buoyed on uncracked supporting beams with s/L = 0.5; (b) depth of crack in supporting beams and cracked bridging beam with depth $a/h = 0.3$

Fig. 7 demonstrates the frequency ratio of cracked crane to uncracked one plotted versus crack position on supporting beams in various crack depths for uncracked (Fig. 7(a)) and cracked (Fig. 7(b)) bridging beam. The graphs provided in Fig. 6 are not symmetrical about the beam middle as those given in Fig. 6. This is a typical effect of crack in supporting beams on fundamental frequency of the overhead crane. Moreover, it is observed in Fig. 7(b) that the horizontal line corresponding to uncracked supporting beams represents maximal change in the frequency due to crack of 30% depth occurred in bridging beam as shown in Fig. 5(a).

Fig. 8 exhibits the effect of supporting locations on cracked crane's fundamental frequency, where graphs are plotted versus crack position on bridging beam in three cases of supporting beams: (Fig. 8(a)) uncracked, (Fig. 8(b)) cracked at their middles, and (c) cracked at symmetrical positions $e_s/L_s = 1/3$ and $2/3$. Obviously, for the crane with intact supporting beams, the effect is symmetrical regarding both crack position on the

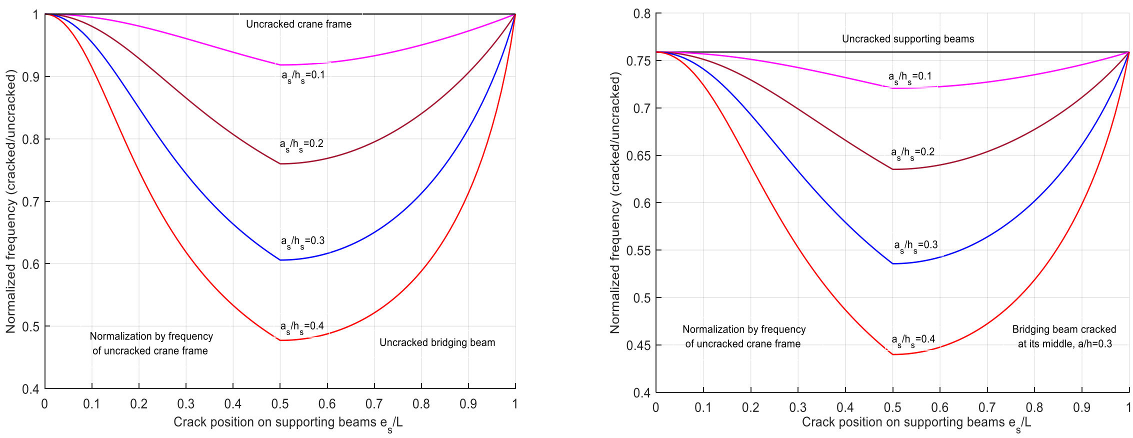

(a) (b)

Fig. 7. Fundamental frequency of overhead crane versus crack position on supporting beams in case of (a) uncracked and (b) cracked bridging beams. Supporting locations are the beams middle and normalization by frequency of uncracked crane

bridging beam and supporting points on the supporting beams. Also, the effect increases as the supporting points move away from the beams' middle to their ends. In case when the supporting beams are cracked the symmetry of the effect is not maintained for supporting locations regardless of where a crack appears in the supporting beams. However, supporting positions on the left of the beam's span ($s < L/2$) make more reduction of the frequency than those on the right ($s > L/2$). Furthermore, it can be seen in Fig. 8(c) that cracks on opposite sides of the supporting beams' middle decrease the frequency reduction due to crack in bridging beam.

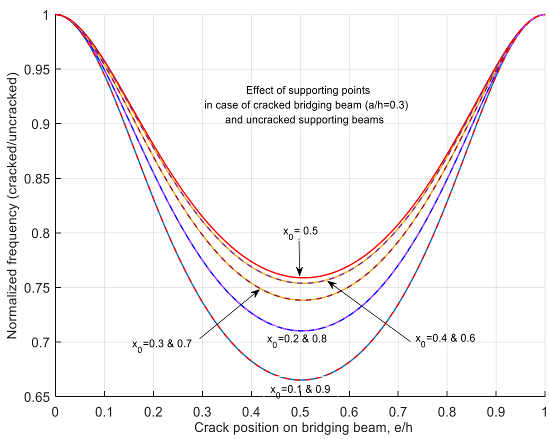

(a)

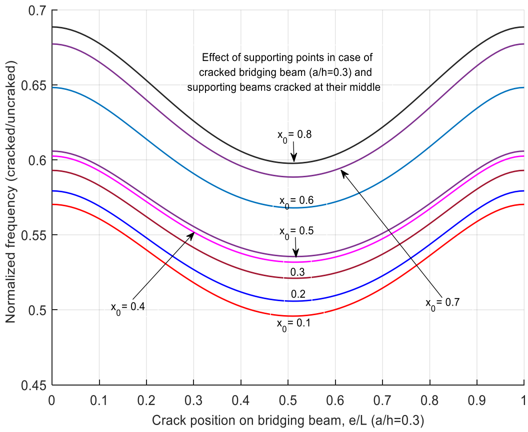

(b)

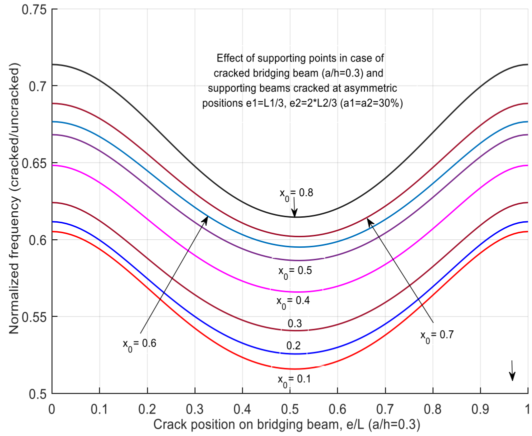

(c)

Fig. 8. Effect of supporting point on fundamental frequency of overhead crane versus crack position on bridging beam (a/h = 0.3) in case of supporting beams (a) uncracked, cracked with depth a_s/L_s= 0.3 (b) at their middle and (c) at the symmetric positions, $e_{AB} = L_s/3$, $e_{CD} = 2L_s/3$

6. CONCLUSIONS

The present study addresses a novel application of the dynamic stiffness method for modal analysis of a 3D-overhead crane consisting mainly of three beam members, one of which is supported by two others. The former member is called the bridging beam, and the two other ones are named after supporting beams. The essential content of the novel application is modeling the 3D-framed crane structure by an equivalent beam with artificial elastic supports of stiffness defined as the dynamic stiffness of the supporting beams.

Therefore, the first result obtained in this study is an expression of dynamic stiffness defined at a position on a cracked beam. This stiffness is a frequency domain function dependent also on the crack parameters and position on beam where the dynamic stiffness has been determined.

Next, vibration shape has been conducted for a cracked beam with elastic supports of stiffness parameters defined above as dynamic stiffness representing the supporting beams with cracks. This provides the vibration shape of an equivalently simplified 3D-framed structure with cracks and used for modal analysis of a cracked overhead crane.

Numerical results obtained herein allow one to draw the following concluding remarks:

- The dynamic stiffness defined as the inverse of the frequency response function for a cracked beam is a consistent description of vibration behavior in cracked beams. This dynamic stiffness of cracked beams can be reliably employed for modeling the supporting beams in a 3D-framed overhead crane.

- The simplified model of the framed overhead crane allows one to capture not only the presence of the supporting beams but also the effect of cracks in these members on the fundamental frequency of the frame crane. It is also observed that cracks in supporting beams may reduce the change in the crane fundamental frequency caused by cracks in the bridging beam. This fact verifies an interaction between cracks in all members of the crane as a total frame structure.

- The effect of positions where the bridging beam is rested on supporting beams on the overhead crane fundamental frequency has also been investigated. It is revealed that the effect is significantly dependent on whether supporting beams are cracked and where they undergo the cracks.

Finally, it can be concluded that the established in this study model can be used for the analysis of the dynamics of the 3D-framed overhead cranes under moving load, the more realistic working state of cranes in general.

DECLARATION OF COMPETING INTEREST

The authors declare that they have no known competing financial interests or personal relationships that could have appeared to influence the work reported in this paper.

ACKNOWLEDGEMENT

This work was completed with financial support from Vietnam Academy of Science and Technology under Grant of number NVCC03.01/24-24.

REFERENCES

[1] E. M. Abdel-Rahman, A. H. Nayfeh, and Z. N. Masoud. Dynamics and control of cranes: A review. *Journal of Vibration and Control*, **9**, (2003), pp. 863–908. https://doi.org/10.1177/1077546303009007007.

[2] M. A. Nasser. Dynamic analysis of cranes. In *Proceedings of IMAC-XIX: A Conference on Structural Dynamics*, (2001), pp. 1592–1599.

[3] M. R. Mojallizadeh, B. Brogliato, and C. Prieur. Modeling and control of overhead cranes: A tutorial overview and perspectives. *Annual Reviews in Control*, **56**, (2023). https://doi.org/10.1016/j.arcontrol.2023.03.002.

[4] D. C. D. Oguamanam, J. S. Hansen, and G. R. Heppler. Dynamic response of an overhead crane system. *Journal of Sound and Vibration*, **213**, (1998), pp. 889–906. https://doi.org/10.1006/jsvi.1998.1564.

[5] H.-H. Lee. Modeling and control of a three-dimensional overhead crane. *Journal of Dynamic Systems, Measurement, and Control*, **120**, (1998), pp. 471–476. https://doi.org/10.1115/1.2801488.

[6] D. C. D. Oguamanam, J. S. Hansen, and G. R. Heppler. Dynamics of a three-dimensional overhead crane system. *Journal of Sound and Vibration*, **242**, (2001), pp. 411–426. https://doi.org/10.1006/jsvi.2000.3375.

[7] J.-J. Wu. Finite element analysis and vibration testing of a three-dimensional crane structure. *Measurement*, **39**, (2006), pp. 740–749. https://doi.org/10.1016/j.measurement.2006.03.002.

[8] T. V. Lien and N. T. Khiem. *The dynamic stiffness method and application in structural analysis and identification*. Construction Publishing House, (2017). (in Vietnamese).

[9] N. T. Khiem and T. V. Lien. The dynamic stiffness matrix method in forced vibration analysis of multiple-cracked beam. *Journal of Sound and Vibration*, **254**, (2002), pp. 541–555. https://doi.org/10.1006/jsvi.2001.4109.

[10] N. T. Khiem and T. T. Hai. *Vibrations in engineering*. VNU Publisher House, (2020). (in Vietnamese).

[11] S. C. Wang, R. S. Shen, T. H. Jin, and S. J. Song. Dynamic behavior analysis and its application in tower crane structure damage identification. *Advanced Materials Research*, **368–373**, (2011), pp. 2478–2482. https://doi.org/10.4028/www.scientific.net/amr.368-373.2478.

[12] D. X. Trong and N. T. Khiem. Modal analysis of tower crane with cracks by the dynamic stiffness method. In *Topics in Modal Analysis & Testing*, Springer International Publishing, Vol. 10, (2017), pp. 11–22. https://doi.org/10.1007/978-3-319-54810-4_2.

[13] D. X. Trong, L. K. Toan, H. T. Ngoc, and N. T. Khiem. Modal analysis of cracked tower crane with an experimental validation. *Vietnam Journal of Science and Technology*, **58**, (2020), pp. 776–788. https://doi.org/10.15625/2525-2518/58/6/15298.

[14] N. T. Khiem, N. M. Tuan, and P. T. B. Lien. Crack identification in beam by antiresonant frequencies. *Vietnam Journal of Mechanics*, **43**, (2021), pp. 389–405. https://doi.org/10.15625/0866-7136/16710.